JOURNAL OF SOLID STATE CHEMISTRY 112, 203–207 (1994)

LETTER TO THE EDITOR

Crystal Structure and Superconductivity of the Mo-Stabilized Sr-Based $YSr_2Cu_{2.7}Mo_{0.3}O_{7-\delta}$ Compound

S. F. Hu,* R. S. Liu,† S. C. Su,‡ D. S. Shy,† and D. A. Jefferson*

*Department of Chemistry, University of Cambridge, Lensfield Road, Cambridge, CB2 1EW, United Kingdom; †Material Research Laboratories, Industrial Technology Research Institute, Hsinchu, Taiwan, Republic of China; and ‡Pacific Electric Wire and Cable Co., Ltd., Tao-Yuan, Taiwan, Republic of China

Communicated by J. M. Honig, June 7, 1994; accepted June 20, 1994

The crystal structure of the Mo-stabilized Sr-based superconductor with nominal composition $YSr_2Cu_{2.7}Mo_{0.3}O_{7-\delta}$ has been analyzed by X-ray powder diffraction (XRD), electron diffraction, and high-resolution electron microscope techniques. The material crystallizes in the space group *P4/mmm*, with lattice parameters $a = 3.8138(2)$ and $c = 11.5204(8)$ Å. In the structure, the Mo ions are exclusively substituted for copper and are located mainly on the planar coordinated [Cu(2)] sites (~24%), with only a small proportion on the chain [Cu(1)] sites (~6%) in the parent $YBa_2Cu_3O_7$ (123-type) structure. A disordering of the hole reservoir layer [Mo(1)/Cu(1)]–O(3) due to the displacement of the oxygen ions [O(3)] from their ideal positions of (0, 0.5, 0) to (0.13, 0.5, 0) was found in the XRD refinement, but neither a superlattice nor any form of intergrowth along the a^* and c^* directions was observed by electron diffraction and high-resolution electron microscopy. The chemical substitution of copper by molybdenum renders the $YSr_2Cu_3O_7$ compound superconducting, with T_c up to 45 K.

1. INTRODUCTION

The effect of chemical substitutions on the superconducting properties of layered cuprates has been one of the most important areas of research in the quest for the real mechanism of high-T_c superconductivity. The $YSr_2Cu_3O_7$ compound is of special interest due to its close crystal structure relationship with the $YBa_2Cu_3O_7$, or 123-type, structure. The replacement of Cu by other metal ions (M) in the structure of $YBa_2Cu_{3-x}M_xO_{7-\delta}$ may occur on two sets of nonequivalent sites, namely, the chain sites, designated Cu(1), and the planar coordinated sites, designated Cu(2) (1–6). Substituent elements with small ionic radii, e.g., Al, Fe, and Co, replace copper on Cu(1), and those of large ionic radii, e.g., Ni and Zn, substitute on the Cu(2) sites. Monophasic $YSr_2Cu_3O_7$, which has a superconducting transition of $T_{c(onset)} = 60$ K and $T_{c(zero)} = 18$ K (7) and some means of producing this phase under less extreme conditions, has frequently been sought. Attempts to stabilize $YSr_2Cu_3O_7$ at normal pressure have generally employed various chemical substitutions, where replacement of Cu by Pb, Li, Al, Ti, V, Cr, Fe, Co, Ga, Ge, Mo, W, and Re have proved to be effective (8–15). However, it has been demonstrated that a relatively small amount of doping in $YBa_2Cu_3O_7$ normally gives rise to a significant decrease in T_c for most substituent elements. Consequently, the exact site-selective substitution for the metal ions in the $YSr_2Cu_3O_7$ structure is of great interest. Here, we describe a determination of the crystal structure of $YSr_2Cu_{2.7}Mo_{0.3}O_7$ using a combination of X-ray powder diffraction (XRD) selected-area electron diffraction (SAED), and high-resolution electron microscopy (HREM). These investigations suggest that the Mo ions are substituted mainly on the Cu(2) planar site but with some substitution on the Cu(1) chain sites to facilitate the formation of the parent $YSr_2Cu_3O_7$ compound.

2. EXPERIMENTAL

Samples in the compositional range $YSr_2Cu_{3-x}Mo_xO_{7-\delta}$ for $0 \le x \le 1$ with steps of $x = 0.1$ were prepared by mixing high-purity powders of CuO, Mo metal, $SrCO_3$, and Y_2O_3. The mixtures were pressed into pellets (10 mm in diameter and 3 mm in thickness) under a pressure of 5 ton/cm^2, which were then heated at a rate of 5°C/min up to 1030°C for 3 hr and cooled down to room temperature at a rate of 1°C/min in an oxygen atmosphere. After this initial reaction, all samples were reground, pressed into pellets, and heated under flowing oxygen for 3 hr at 1040°C, using the same heating and cooling rate.

Powder X-ray diffraction analyses were performed using a Philips PW1820 X-ray diffractometer with Ni-filtered Cu$K\alpha$ radiation. The sampling interval was 0.02° in 2θ,

0022-4596/94 $6.00

and the accumulation time was 10 sec per step. The 2θ range was from 20° to 100°. The datasets were refined using the Rietveld analysis computer program DBWS-9006 provided by Wiles and Young (16). XRD traces indicated that a truly monophasic sample was only obtained for $x = 0.3$, and consequently it was this sample which was selected for analysis using profile refinement. For the HREM studies, a modified side-entry goniometer system was employed in a JEOL-200CX microscope operating at 200 kV, with electron-optical parameter $C_s = 0.41$ mm and $C_c = 0.98$ mm, these corresponding to resolution figures of 0.185 nm (interpretable) and 0.170 nm (absolute), respectively (17). The SAED patterns were obtained in the same microscope equipped with a ±15° double tilting goniometer stage. Powdered specimens for HREM and SAED examination were ground in an agate mortar with acetone for a few minutes, and a drop of suspension was placed on a copper grid upon which a holey carbon film had been deposited. Micrographs were recorded at a magnification of ca. 450,000×, after careful correction of beam alignment and residual astigmatism by observing the granularity of the holey carbon film. As an aid to image interpretation, computer image simulations employing the multislice method (18, 19) were carried out using the commercially available CERIUS HRTEM programs. A standard four-probe method was used for the electrical resistance measurements. Electrical contacts to the sample were made by fine copper wires with a conductive silver paint, the applied current being 1 mA, and the temperature was recorded using a calibrated Pt sensor located adjacent to the sample.

3. RESULTS AND DISCUSSION

The observed XRD diffraction data, along with the diffraction pattern, of $YSr_2Cu_{2.7}Mo_{0.3}O_7$ are shown in Fig. 1. Experimental data are shown by crosses ("+"), and the solid curve represents the calculated profiles based on the *P4/mmm* space group. Thermal parameters (B) were assumed to be isotropic. The short vertical lines mark the positions of possible Bragg reflections. The lower portion of the figure shows the difference between calculated and observed diffraction profiles, and the overall agreement demonstrates that the structure based on this space group is a good approximation to that actually producing the experimental diffraction data. The numerical results of this structural refinements are shown in Table 1. The refined lattice constants were $a = 3.8138(2)$ and $c = 11.5204(8)$ Å, the final R factors being $R_p = 2.52$, $R_{wp} = 3.32$, and $R_I = 10.50\%$. The reasonably good fit between the observed and the calculated patterns, together with the small R factors, indicates the reliability of the analysis.

Site occupancy refinement indicated that the chemical

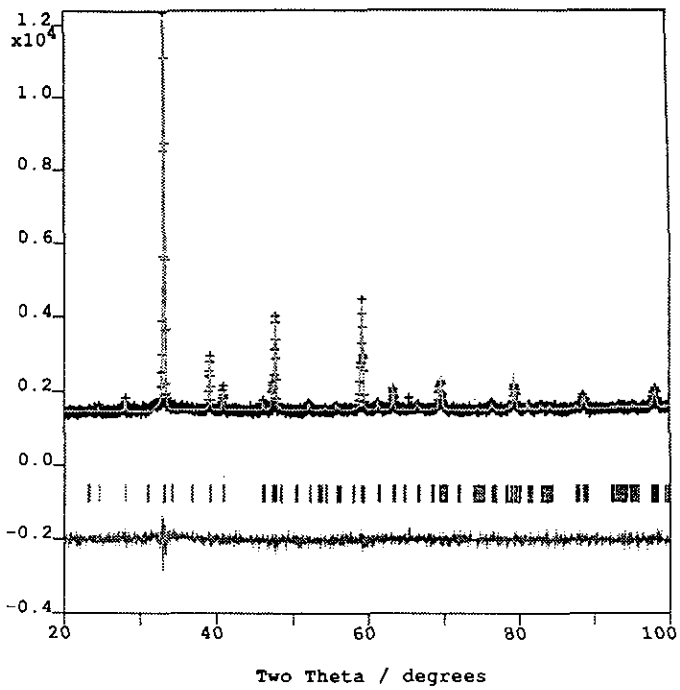

FIG. 1. The observed (crosses), calculated (solid line), and difference powder X-ray diffraction patterns of the sample with a nominal composition of $YSr_2Cu_{2.7}Mo_{0.3}O_7$.

substitution of the Mo ions for the Cu ions in $YSr_2Cu_3O_7$ was found to occur mainly on the planar [Cu(2)] sites (~24%) but with minor substitution on the chain [Cu(1)] sites (~6%) in the $YBa_2Cu_3O_7$ (123-type) parent structure. This pattern of chemical substitution of the Mo ions into

TABLE 1

Positional[a] and Thermal Parameters B (Å²) and Site Occupancies (g) of the Sample Having the Nominal Composition ($Mo_{0.3}Cu_{0.7}$) $Sr_2YCu_2O_7$

Atom	Site	x	y	z	B	g
Mo(1)	1*a*	0	0	0	1.0(6)	0.06(8)
Cu(1)	1*a*	0	0	0	1.0(6)	0.94(8)
Sr	2*h*	0.5	0.5	0.1920(7)	2.9(2)	2.0
Y	1*d*	0.5	0.5	0.5	1.6(3)	1.0
Mo(2)	2*g*	0	0	0.357(1)	3.8(3)	0.48(8)
Cu(2)	2*g*	0	0	0.357(1)	3.8(3)	1.52(8)
O(1)	4*i*	0	0.5	0.376(2)	3.0(8)	4.0
O(2)	2*g*	0	0	0.160(4)	2.5(9)	2.0
O(3)[b]	4*n*	0.13(5)	0.5	0	8(5)	0.25
$a = 3.8138(2)$ Å						
$c = 11.5204(8)$ Å						
$R_p = 2.52\%$						
$R_{wp} = 3.32\%$						
$R_I = 10.50\%$						

[a] Space group *P4/mmm* (No. 123).
[b] Refined off ideal site 2*f*, (0, 0.5, 0).

TABLE 2

Selected Interatomic Distances (Å) and Angles (°) for the Compound Having the Nominal Composition of $(Mo_{0.3}Cu_{0.7})Sr_2YCu_2O_7$

Bonds	Distances (Å)	K^a
Mo(1)/Cu(1)–O(2)	1.847	2
–O(3)	1.966	8
Mo(2)/Cu(2)–O(1)	1.920	4
–O(2)	2.263	1
Y–O(1)	2.381	8
Sr–O(1)	2.854	4
–O(2)	2.721	4
–O(3)	2.632	4
Mo(2)/Cu(2)–Mo(2)/Cu(2)	3.299	Intersheet
Bonds	**Angle (degrees)**	
O(1)–Mo(2)/Cu(2)–O(1)	89.2173	
O(1)–Mo(2)/Cu(2)–O(1)	166.5580	
O(1)–Mo(2)/Cu(2)–O(2)	96.7121	

[a] K is the number of equivalent bonds.

both Cu sites was also observed using Raman spectroscopy (14) in the same compound synthesized under hydrostatic pressure. A disordering of the hole reservoir layer [Mo(1)/Cu(1)]–O(3) due to the displacement of the oxygen ions [O(3)] from their ideal $2f$, (0, 0.5, 0), sites to $4n$, (0.13, 0.5, 0), sites was observed in the positional refinement.

Selected interatomic distances and angles for the $YSr_2Cu_{2.7}Mo_{0.3}O_7$ sample are listed in Table 2. The bond angle of O(1)–[Mo(2)/Cu(2)]–O(1) is 166.6°, confirming that the conducting CuO_2 planes are buckled in a similar way to that found in $YBa_2Cu_3O_{7-\delta}$. The Mo(2)/Cu(2) site is coordinated by five oxygen atoms in a pyramidal configuration with a long apical distance, [Mo(2)/Cu(2)]–O(2) = 2.263 Å, but having much shorter in-plane distances, namely [Mo(2)/Cu(2)]–O(1) = 1.920 Å. This coordination of Mo(2)/Cu(2) is similar to that found in the more usual cuprate superconductors. The distances [Mo(2)/Cu(2)]–O(1) and [Mo(2)/Cu(2)]–O(2) found in $YSr_2Cu_{2.7}Mo_{0.3}O_7$ are close to those reported for $(Y_{0.7}Ca_{0.3})Sr_2(Cu_{2.35}Pb_{0.65})O_7$, which has 1.916 Å for the in-plane bonds and 2.343 Å for the apical distance (11). A schematic representation of the crystal structure of $YSr_2Cu_{2.7}Mo_{0.3}O_7$ is shown in Fig. 2.

In Fig. 3 we show the SAED pattern (inset in the upper right-hand corner) and HREM image along the [010] direction with a computer-simulated image inset in the lower left-hand corner taken from the $YSr_2Cu_{2.7}Mo_{0.3}O_7$ sample. The specimen thickness and objective lens defocus used for the simulation were 30.5 and −1125 Å, respectively. The lattice constants a and c derived from the SAED pattern are identical with those resulting from the XRD refinement. Moreover, no superlattice spots were observed in the SAED pattern, which indicates that the material is basically homogeneous without any ordering of defects. The HREM image of the sample viewed down [010] is shown in Fig. 3, this being recorded at an objective lens defocus well beyond the so-called "Scherzer" value, so that the cations in the structure appear as white dots. One can observe two sets of triple rows containing alternating white dots. Image simulations from the model structure indicate that the brighter first set can be correlated with the layer sequence "SrO–[Mo(1)/Cu(1)]O(3)–SrO" (the positions of the Mo(1)/Cu(1) atoms being indicated by arrows), whereas the second, weaker set corresponds to the layer sequence "[Mo(2)/Cu(2)]O_2–Y–[Mo(2)/Cu(2)]O_2." This sequence of layers, ... [Mo(1)/Cu(1)]O(3)–SrO–[Mo(2)/Cu(2)]O_2–Y–[Mo(2)/Cu(2)]O_2–SrO–[Mo(1)/Cu(1)]O(3) ..., is consistent with the proposed "123"-type structure. Agreement between the calculated image, shown in the lower left-hand corner of Fig. 3, and the experimental micrograph is good. An almost perfect stacking sequence was observed throughout the structure, unlike the case of the thallium cuprates (20), which almost invariably display intergrowths of phases with different layers of thickness.

In Fig. 4 we show the temperature dependence of the resistance of the $YSr_2Cu_{2.3}Mo_{0.3}O_7$ sample. The sample exhibits metallic behavior in the normal state with superconducting transition temperatures of $T_{c(onset)}$ = 50,

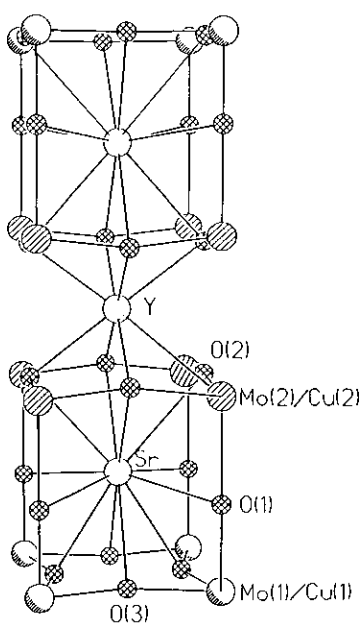

FIG. 2. The crystal structure of the $YSr_2Cu_{2.7}Mo_{0.3}O_7$ compound.

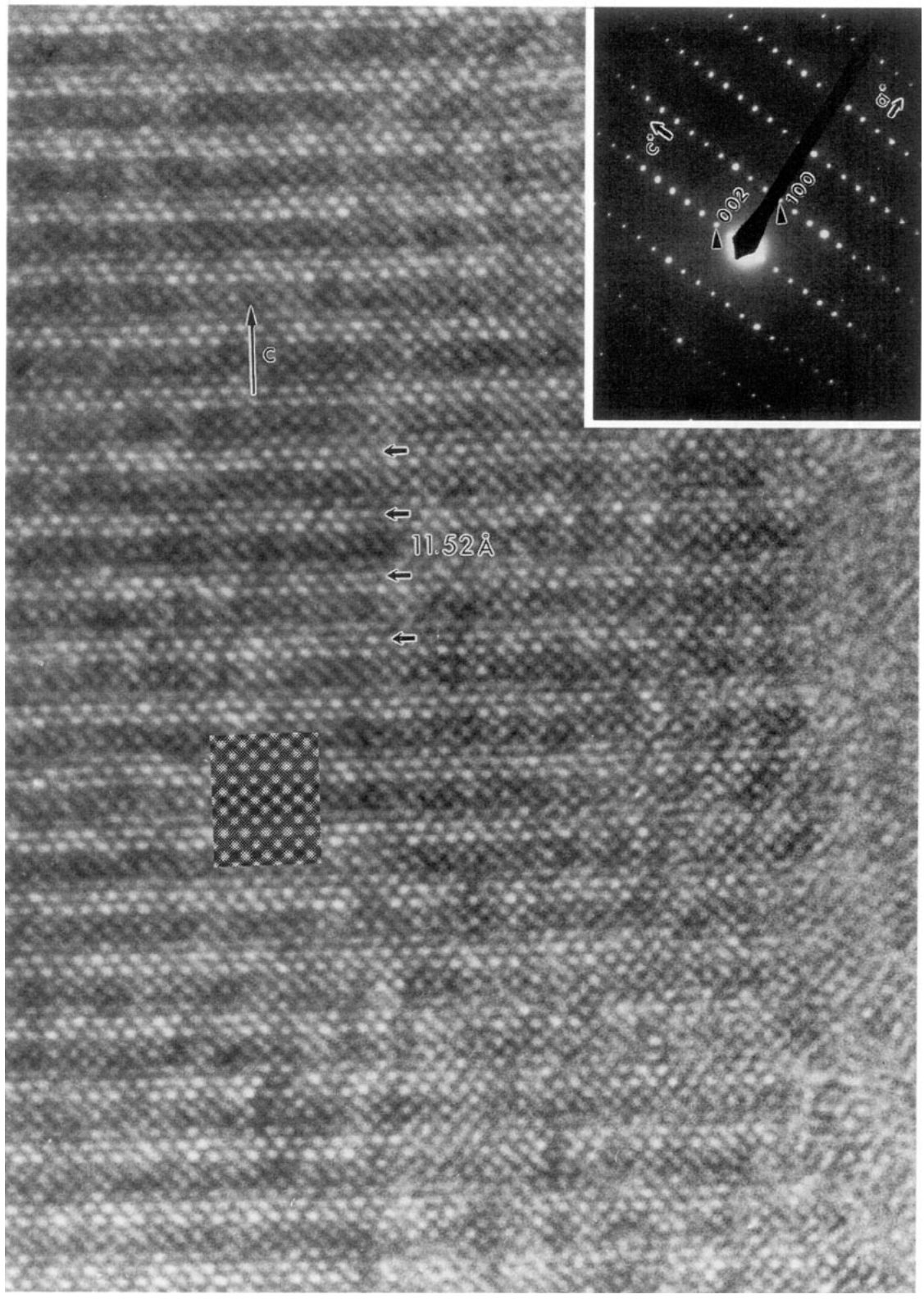

FIG. 3. SAED pattern (inset of the upper right-hand corner) and HREM image along the [010] direction with a computer-simulated image inset in the lower left-hand corner taken from the $YSr_2Cu_{2.7}Mo_{0.3}O_7$ sample. The specimen thickness and objective lens defocus used for the simulation were 30.5 and -1125 Å, respectively.

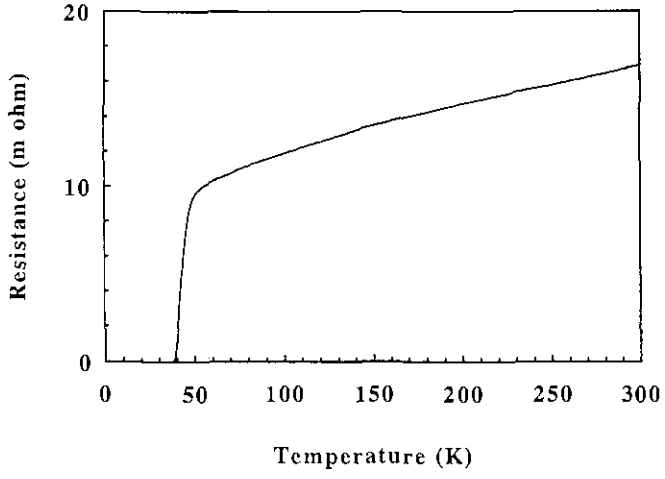

FIG. 4. Temperature dependence of resistance of the $YSr_2Cu_{2.3}Mo_{0.3}O_7$ sample.

$T_{c(midpoint)} = 45$, and $T_{c(zero)} = 37$ K. In comparison, the pure $YSr_2Cu_3O_7$ phase, when prepared at a high oxygen pressure of 7 GPa, only has a semiconducting behavior in the normal state with a very broad superconducting transition of $T_{c(onset)} \sim 60$, $T_{c(midpoint)} \sim 49$, and $T_{c(zero)} \sim 18$ K (7). This result indicates that the chemical substitution of Mo for Cu in $YSr_2Cu_3O_7$ does not only stabilize the crystal structure at more conventional pressures but also improves the superconducting properties.

In summary, we have demonstrated that the crystal structure of $YSr_2Cu_{2.7}Mo_{0.3}O_7$ as revealed by X-ray powder diffraction, selected-area electron diffraction, and high-resolution electron microscopy is of the expected 123 type. Detailed refinement suggests that the Mo ions are substituted mainly on the Cu(2) planar coordinated site but with some replacement of copper also on the Cu(1) chain sites. The displacement of the O(3) ions from their ideal positions was also established. In addition, chemical substitution of copper by molybdenum is found to improve the superconducting properties of the $YSr_2Cu_3O_7$ parent compound.

ACKNOWLEDGMENTS

The authors thank the Ministry of Economic Affairs of the Republic of China for the financial support. One of us (S.F.H.) also thanks Girton College (Cambridge) and the Cambridge Overseas Trust for financial support. Electron microscope facilities were provided by the SERC (UK), and this is gratefully acknowledged.

REFERENCES

1. J. M. Tarascon, P. Barboux, P. F. Miceli, L. H. Greene, G. W. Hull, M. Eibschuttz, and S. A. Sunshine, *Phys. Rev. B* **37,** 7459 (1988).
2. T. Kistenmacher, *Phys. Rev. B* **38,** 8862 (1988).
3. J. F. Bringley, T. M. Chen, B. Averill, K. M. Wong, and S. J. Poon, *Phys. Rev. B* **38,** 2432 (1988).
4. G. Xiao, M. Z. Cieplak, D. Musser, A. Gavrin, F. H. Streitz, C. L. Chien, J. J. Rhyne, and J. A. Gotaas, *Nature* **332,** 238 (1988).
5. T. Takabatake and M. Ishikawa, *Solid State Commun.* **66,** 354 (1988).
6. Y. Xu, R. Sabatini, A. Moodenbaugh, Y. Zhu, S. Shyu, M. Suenaga, K. Dennis, and R. McCallum, *Physica C* **169,** 205 (1988).
7. B. Okai, *Jpn. J. Appl. Phys.* **29,** L2180 (1990).
8. R. S. Liu, S. F. Hu, I. Gameson, P. P. Edwards, A. Maignan, T. Rouillon, D. Groult, and B. Raveau, *J. Solid State Chem.* **93,** 276 (1991).
9. A. Maignan, T. Rouillon, D. Groult, J. Provost, M. Hervieu, C. Michel, B. Raceau, R. S. Liu, and P. P. Edwards, *Physica C* **177,** 461 (1991).
10. S. F. Hu, D. A. Jefferson, R. S. Liu, and P. P. Edwards, *J. Solid State Chem.* **96,** 455 (1992).
11. T. Maeda, K. Sakuyama, F. Izumi, H. Yamauchi, H. Asano, and S. Tanaka, *Physica C* **175,** 393 (1991).
12. P. R. Slater and C. Greaves, *Physica C* **180,** 299 (1991).
13. T. Den and T. Kobayashi, *Physica C* **196,** 141 (1992).
14. Q. Xiong, Y. Q. Wang, J. W. Chu, Y. Y. Sun, K. Matsuishi, H. H. Feng, P. H. Hor, and C. W. Chu, *Physica C* **198,** 70 (1992).
15. Y. Zhou, F. Shi, H. K. Liu, C. Andrikidis, and S. X. Dou, *Physica C* **212,** 451 (1993).
16. D. B. Wiles and R. A. Young, *J. Appl. Crystallogr.* **14,** 149 (1981).
17. D. A. Jefferson, J. M. Thomas, G. R. Millward, K. Tsuno, A. Harriman, and R. D. Brydson, *Nature* **323,** 428 (1986).
18. J. M. Cowley and A. F. Moodie, *Acta Crystallogr.* **16,** 609 (1957).
19. P. Goodman and A. F. Moodie, *Acta Crystallogr. Sect. A* **30,** 280 (1974).
20. M. Hervieu, C. Michel, and B. Raveau, *J. Less-Common Met.* **150,** 59 (1989).